Chemistry–A European Journal | Concept
doi.org/10.1002/chem.202302251
Chemistry Europe
European Chemical Societies Publishing

www.chemeurj.org

Boosting the Oxygen Evolution Activity of FeNi Oxides/Hydroxides by Molecular and Atomic Engineering

Eliana S. Da Silva[+],[a] Aureliano Macili[+],[a] Roger Bofill,[a] Jordi García-Antón,[a] Xavier Sala,[a] and Laia Francàs*[a]

FeNi oxides/hydroxides are the best performing catalysts for oxidizing water at basic pH. Consequently, their improvement is the cornerstone to develop more efficient artificial photosynthetic systems. During the last 5 years different reports have demonstrated an enhancement of their activity by engineering their structures via: (1) modulation of the number of oxygen, iron and nickel vacancies; (2) single atoms (SAs) doping with metals such as Au, Ir, Ru and Pt; and (3) modification of their surface using organic ligands. All these strategies have led to more active and stable electrocatalysts for oxygen evolution rection (OER). In this Concept, we critically analyze these strategies using the most relevant examples.

1. Introduction

Storing green electricity in the form of chemical bonds is a promising approach to generate green and renewable fuels and help in the decarbonization of the environment. One of the most studied and promising strategies to achieve this goal is the extraction of electrons from water to use them to generate a fuel such as hydrogen, in the so-called water splitting process,[1,2] or to form reduced carbon molecules, e.g. ethanol, in the well-known CO_2 reduction reaction.[3,4] Independently of the final product, these processes (water splitting and CO_2 reduction) have in common the oxidative part, in which water is oxidized to oxygen. This is a thermodynamic uphill ($\Delta G =$ 475 kJ/mol, pH = 0) and kinetically slow reaction that is proposed to be, in most cases, the bottleneck of the whole process, involving the extraction of 4 electrons and 4 protons from 2 water molecules to generate an oxygen-oxygen double bound.[5,6] This reaction usually takes place through a 4 steps pathway [Eqs. (1)–(4)]:[7]

$$H_2O(l) + * \rightarrow HO^* + H^+ + e^- \quad (1)$$

$$HO^* \rightarrow O^* + H^+ + e^- \quad (2)$$

$$O^* + H_2O(l) \rightarrow HOO^* + H^+ + e^- \quad (3)$$

$$HOO^* \rightarrow * + O_2 + H^+ + e^- \quad (4)$$

where * is the active site on the surface of the catalyst. However, despite this being one of the most accepted mechanisms, other pathways can also be considered.[8,9]

In this field, a lot of effort has been devoted to find an earth abundant active catalyst towards the oxygen evolution reaction (OER).[10] Currently, the best performing OER catalysts in alkaline media are those based on NiFe oxides/hydroxides.[11,12] Even though the positive effect of Fe^{3+} incorporation into Ni oxide/hydroxide-based anodes for OER was reported by Corrigan in 1987,[13] it has not been until the last decade that this field has exponentially grown, with the obtaining of different NiFe based electrocatalysts. Since the revisiting of this effect by Boettcher and coworkers in 2012,[14] a great number of studies have investigated this phenomenon.[15–19] However, they did not reach a clear picture on the exact role of Fe^{3+} in the OER catalysis.[20]

Catalysts based on NiFe oxides/hydroxides can be prepared following different methodologies. Among them, the most widely employed are: (1) coprecipitation,[21,22] (2) electrodeposition[23–27] and (3) hydrothermal synthesis.[28–30] Each synthetic methodology yields different structures with different catalytic behavior.[31] Among all the different structures existing for NiFe oxides/hydroxides, in this Concept we will focus on examples dealing with layered double hydroxides (LDHs),[32–43] nanostructured alloys[44,45] and coordination polymers.[46] In particular, NiFe LDH are widespread structures leading to highly active electrocatalysts for OER. Their structure consists in brucite-like layers of Ni(II) and Fe(III) mixtures stacked with interlayer anions and hydration water molecules (Figure 1).[47–49]

In addition to Fe^{3+} incorporation, the scientific community has also been studying other strategies to improve the OER performance of NiFe oxide/hydroxide catalysts. (1) Increasing the number of active sites by generating an amorphous catalyst,[50] 2D layers[51] or 3D structures.[52] (2) Generating heterostructures by coupling NiFe species with other electrocatalysts,[53–55] or changing the conductive support to improve the electronic properties.[56–60] (3) Changing the intercalated anions when using NiFe LDHs to improve the amount of

[a] Dr. E. S. Da Silva,[+] A. Macili,[+] Dr. R. Bofill, Dr. J. García-Antón, Dr. X. Sala, Dr. L. Francàs
Departament de Química
Universitat Autònoma de Barcelona
Cerdanyola del Vallès, 08193 Barcelona (Spain)
E-mail: Laia.Francas@uab.cat

[+] These authors contributed equally to this work.

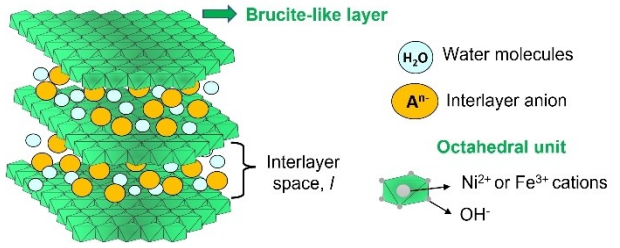

Figure 1. Schematic representation of a NiFe LDH structure.

exposed active sites, lowering the charge transfer resistance and inducing a better contact with the electrolyte.[61–64] (4) Doping with other elements, either metals and non-metals, thus changing the intrinsic properties of the catalyst.[65–67] (5) Introducing cationic and/or anionic vacancies.[32–35,68] (6) Incorporating single atoms (SAs) into the catalyst structure.[37–41,44] (7) Using organic molecules to modulate the coordination sphere of the active species.[42,43,45,46] In this Concept, we will discuss the last three methodologies that atomically or molecularly modify the structure of the NiFe oxide/hydroxide catalysts. These strategies allow to rationally tune the electronic properties of the active sites, and consequently to modulate their reactivity. The most relevant examples of each strategy and their corresponding benchmarking overpotential in OER are summarized in Table 1.

Table 1. NiFe LDHs, NiFe coordination polymers and NiO materials atomically and/or molecularly modified with their corresponding OER benchmarking overpotential at a current density of 10 mA/cm^2 (unless otherwise indicated) discussed in this work. V_O, oxygen vacancies; V_{Fe}, Fe vacancies; V_{Ni}, Ni vacancies; SAs, single atoms; EWD, electron withdrawing; FBS, nonafluoro-1-butanesulphonate.

Entry	Strategy	Details	η_{10} [mA/cm^2]	Ref.
1	Vacancies	V_O, V_{Ni} and V_{Fe}	205	[32]
2	Vacancies	V_{Ni}	200 (20 mA/cm^2)	[33]
3	Vacancies	V_{Ni}	229	[34]
4	Vacancies	V_{Fe}	245	[34]
5	Vacancies	V_O	195	[35]
6	Vacancies	V_O, V_{Ni} and V_{Fe}	230	[68]
7	SAs	Au	210	[37]
8	SAs	Ir	200	[44]
9	SAs + vacancies	Ru + V_{Fe}	189	[38]
10	SAs	Ru	194	[40]
11	SAs	Pt	270	[39]
12	SAs	Pt	243	[41]
13	Ligand	Terephthalic Acid (Carboxylate)	188	[46]
14	Ligand	C_6F_5 (most EWD ligand)	268	[45]
15	Ligand	FBS	199	[42]
16	Ligand + doping	LiAc	159	[43]
17	Vacancies + structural defects	V_O + Ni^{3+} defects + porosity	170	[36]

2. Vacancies Modulation

It is widely accepted that atomic scale defects (cationic and oxygen vacancies) enhance OER in metal oxide catalysts.[33,69,70] In the case of oxygen (anionic) vacancies, it is known that they affect both the surface and bulk electronic structure. The former will modulate the adsorption energy of the different reaction intermediates, while the latter can increase the covalency of the metal-oxygen bond, which can change the reaction mechanism and improve the electronic conductivity. In NiFe oxides/hydroxides, these vacancies can be M(II) (V_{Ni}) or M(III) (V_{Fe}) in nature, each of them leading to different effects. Cationic vacancies, specially V_{Ni}, have been reported to increase the stability of NiFe-LDH in two ways: by allowing the accommodation of the lattice distortion caused by the presence of nearby Fe(III) sites, and by increasing the binding energy of neighboring Fe–O moieties.[71] On the other hand, V_{Fe} modulate the electronic structure of the materials and are the main responsible for the improved intermediate binding energies leading to an enhanced OER performance.[71] Focusing on NiFe oxides/hydroxides for OER, different strategies have been used to prepare defective materials: (1) modified synthetic methods to produce materials rich in both cationic and anionic vacancies,[68,72–74] (2) decomposition of molecularly well-defined precursors such as Prussian blue,[75] (3) post-synthetic treatments by (a) introducing cationic defects by synthesizing NiFeZn or NiFeAl oxohydroxides and then etching the third metal (Zn^{2+} or Al^{3+}) to selectively produce Ni (M(II), V_{Ni}) or Fe (M(III), V_{Fe}) vacancies, respectively,[33,34] (b) by introducing anionic defects by reducing the pristine materials with a reductive agent such as $NaBH_4$[35,76] or via flame treatment,[77] and (c) by introducing both cationic and anionic defects by a fluorination-enabled surface reconstruction after electrochemical activation,[78] or by combination of strategies 3a and 3b (entry 1,Table 1),[32] or finally (4) doping with non-metallic anions such as B, S and P in negative oxidation states to introduce different amounts of oxygen vacancies (V_O).[79]

Cationic vacancies: In two independent works,[33,34] the authors selectively generated M(III) or M(II) vacancies by etching Al in NiFeAl or Zn in NiFeZn, respectively (Figure 2a). Both works found that both vacancy-containing catalysts were more active than the pristine counterpart and that the catalyst containing V_{Ni} outperformed the one containing V_{Fe} (entries 2, 3 and 4 in Table 1 and Figure 2b). Sun and co-workers[33] associated this different behavior to the different unsaturated sites generated by the vacancies: V_{Fe} leads to Ni(II)–O–Ni(II) unsaturated sites, which are less active than the Ni(II)–O–Fe(III) unsaturated sites generated by V_{Ni}. In addition, DFT calculations indicate that both cationic vacancies favor the deprotonation step in OER, enhancing their activity (equation 2 and Figure 2c).[33,34]

Anionic vacancies: Lin and co-workers reported a material rich in oxygen vacancies due to the post-synthetic treatment of

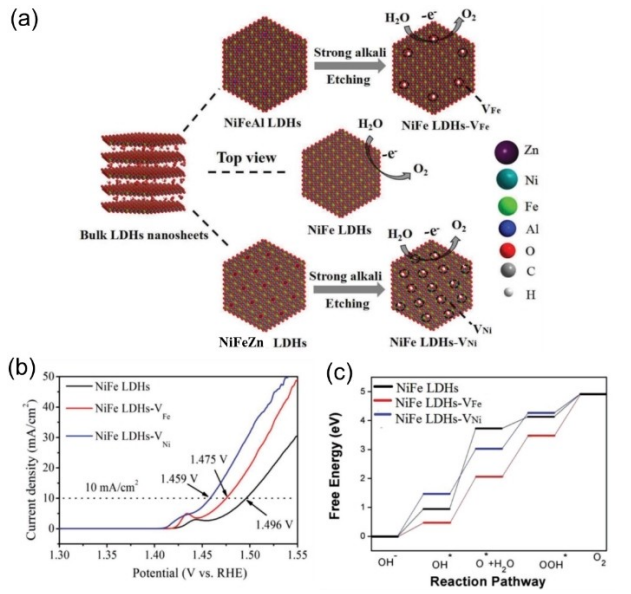

Figure 2. (a) The synthesis of NiFe LDHs-V_{Fe} and NiFe LDHs-V_{Ni} by strong alkali etching. (b) LSVs for OER under 1 M KOH of NiFe, NiFe-V_{Fe} and NiFe-V_{Ni} LDHs at a scan rate of 5 $mV \cdot s^{-1}$. (c) The free energy profile for the OER pathways calculated by DFT for the three systems. Reproduced with permission.[34] Copyright 2018, Wiley-VCH.

a NiFe LDH with $NaBH_4$, which presented an improved performance compared to the pristine material (Figure 3a, entry 5, Table 1).[35] DFT calculations demonstrate that this enhancement is due to a reduction of the energy barrier of the formation of *O from *OH (equation 2 and Figure 3b), in addition to the conductivity improvement due to a decrease in the band gap. Also, Ahn and coworkers studied the evolution of oxygen vacancies under turnover conditions.[79] A decrease of the population of vacancies over time was observed, which was correlated with a decrease in the catalyst OER performance along time.

Both anionic and cationic vacancies: The work reported by Zhang and co-workers describes the preparation of defect-rich ultrafine monolayer NiFe LDH nanosheets (entry 6, Table 1) outperforming the non-defective non-ultrafine monolayer ones.[68] According to density of states depicted by DFT

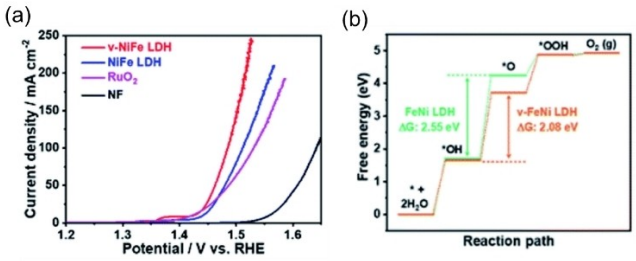

Figure 3. (a) LSVs for OER under 1 M KOH of NiFe LDH-V_O (red curve) and its pristine NiFe LDH counterpart (blue curve) compared to the blanks of commercial RuO_2 (purple curve) and commercial Ni foam, NF (black curve). (b) Theoretical OER Gibbs free energy diagrams for NiFe LDH (green) and NiFe LDH-V_O (orange). Reproduced with permission.[35] Copyright 2021, Royal Society of Chemistry.

calculations, the highly defective nature of the material confers it semimetal character due to the disappearance of the bandgap. The DFT calculations also demonstrate that both metal and oxygen vacancies, present in the ultrathin defective NiFe LDH, enhance its ability to bond OH* (equation 1), enhancing its catalytic performance.[68]

In short, selectively introducing atomic V_{Fe}, V_{Ni} and/or V_O vacancies can rationally increase the electrocatalytic activity of NiFe oxides/hydroxides towards OER by the combination of different positive effects of each defect: V_{Fe} and V_{Ni} will improve the deprotonation step in the mechanism (equation 2) and V_{Ni}, in addition, will generate more active Ni–O–Fe unsaturated sites, while V_O will reduce the energy barrier of the formation of *O from *OH (equation 2) and increase the conductivity of the materials. Moreover, the combination of all these defects will lead to a more continuous density of states, reducing the bandgap and yielding even higher conductivity due to an increased metallic nature of the materials.

3. Doping with Single Atoms (SAs)

Metal doping is a well-known strategy to change the electronic structure and the energy bonding of the key catalytic intermediates formed for a given metal/metal oxide catalyst.[80] When this doping takes place at the atomic scale (introducing single atoms into a metal/metal oxide matrix), the strong metal-matrix interactions arising from interfacial bonding confers unique properties and catalytic performance to the doped catalyst.[81] In this context, the incorporation of Au, Ir, Ru and Pt single atoms (SAs) onto NiFe oxides/hydroxides has been recently used to improve their OER catalytic activity thanks to the strong interaction of the incorporated SAs with the surrounding metal atoms, where the final effect of the SAs strongly depends on the synthetic procedure employed. The incorporation of these SAs onto NiFe oxides/hydroxides can improve the catalyst activity in three ways: (1) the SAs are the only active sites,[82,83] (2) the SAs strongly interact with the NiFe oxide/hydroxides, changing their properties and leading to more active Ni/Fe active sites,[37,39,41,44] (3) both the incorporated SAs and the NiFe oxide/hydroxides directly contribute to the OER activity under operational conditions.[38,40] In this work we will mainly focus on the last two cases, were the SAs improve the catalytic ability of the Ni and Fe metal centers.

Au SAs supported onto a NiFe LDH have been prepared through electrodeposition by Zhang et al.[37] As shown by DFT simulations, Au SAs play a critical role in tuning the charge distribution of active Fe atoms (considered the active sites, see Figure 4) via electron transfer, provoking a change of rate determine step (RDS) from equation 2 in the pristine material to equation 3 in the modified one. This is because the strong interaction between the Fe atoms and the Au lowers the energy for the formation of O* from HO* (equation 2). These changes lead to a lower OER overpotential (entry 7, Table 1) in comparison to the pristine electrocatalyst.

Luo et al.[44] have described an easy and simple strategy to anchor *Ir* SAs (characterized by EXAFS, XPS and HAADF-STEM)

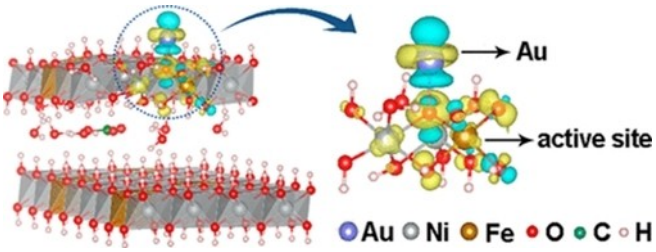

Figure 4. Differential charge densities of NiFe LDH with (top) and without (bottom) one Au atom when one O atom is adsorbed on the Fe site. Isosurface value is 0.004 e·Å^{-3}. Yellow and blue contours represent electron accumulation and depletion, respectively. Reproduced with permission.[37] Copyright © 2018 American Chemical Society.

on three-dimensional (3D) amorphous NiFe/Ni core-shell nanowire@nanosheets ($NiFeIr_{0.03}$/Ni NW@NSs) by a one-step reduction via a kinetically controlled process. The presence of only Ni-based hydroxides with disordered crystalline structure in the shell area and the existence of only single Ir atoms uniformly anchored in the core area contribute to obtain a material with larger surface area, increased number of active sites and better electron transfer properties. DFT calculations suggest that the improved intrinsic activity of the as-prepared $NiFeIr_{0.03}$/Ni NW@NSs (entry 8, Table 1) is due to the synergistic effect between Ir SAs and the Ni active sites in the NiFe nanostructure; as a consequence, the energetic barrier of the RDS (equation 3) is reduced, leading to a lower onset potential than the pristine material.

Ru SAs have been incorporated into NiFe oxide/hydroxide LDHs following two different strategies. Firstly, Zhai and co-workers[38] incorporated Ru SAs into defective NiFe LDH via electrodeposition followed by alkaline etching. This allowed to remove Al from the NiFeAl LDH precursor and obtain defective NiFe LDH nanosheets with Ru SAs. The authors found that the precise regulation of local coordination environments of the active sites and the presence of abundant defects in the LDH (see previous section) contribute to promote the OER performance in alkaline media (entry 9, Table 1) by stabilizing Ru atoms on the LDH support, thus outperforming the catalytic performance of the non-defective NiFe LDH (Figure 5). Both experimental and theoretical studies confirm that the intimate electronic interaction between Ru SAs (considered the main active sites) and defect-rich NiFe LDH nanosheets is beneficial to accelerate the reaction kinetics, promoting the OER. In addition to Ru SAs, the participation of Ni sites as catalytic centers was confirmed under long-term electrolysis conditions. In a second example, Ru SAs were anchored onto Fe^{2+} ion-doped NiFe LDH (Ru/$NiFe^{2+}$Fe LDH).[40] The prepared catalyst displays improved activity and stability on both Ru sites and NiFe LDH, ascribed (through DFT calculations) to the strong electronic interaction between Ru and Fe^{2+}, which lowers the oxidation state of Ru and enhances the Fe–O bond strength (entry 10, Table 1), both being considered the active sites.

Pt atoms have also been introduced as SAs onto NiFe LDHs following two different approaches. In 2021, Chen and co-authors[39] used a two-step synthetic approach to intercalate Pt SAs in a Ni_3Fe–CO_3^{2-} LDH through anionic exchange and space-confined electroreduction. The resulting electrocatalyst presents an improved OER activity (entry 11, Table 1) compared to the bare NiFe LDH. Experimental and DFT studies show that the interlayer Pt SAs increase the Ni valence state and shorten the Ni/Fe–O bonds, contributing to increase the number of active sites ($Ni^{2+\delta}$–O–$Fe^{3+\zeta}$) during the active phase transition, from Ni_3Fe LDH Pt SAs to $Ni_3{}^{2+\delta}Fe^{3+\zeta}O_xH_y$ Pt SAs, optimizing the overall OER activity. Very recently, Wang et al.[41] have described the fabrication of massive single-atom Pt-loaded α–$Ni_xFe_{1-x}(OH)_2$ electrocatalysts via a facile in situ oxidation strategy with H_2PtCl_6. During the synthetic process, Fe cationic vacancies are generated at the surface of the hydroxide, whereas the Pt SAs are anchored *in situ* on these vacancies with a massive loading of ca. 6.15 wt%. DFT calculations show that the Pt single atoms regulate the electronic structure of the NiFe LDH at the Fe cationic vacancies, activating the neighbouring Ni (considered the active centres) and Fe atoms to accelerate the reaction kinetics, thus optimizing the OER performance (entry 12, Table 1).

To summarize, the SAs introduced in the NiFe oxide/hydroxides catalysts strongly interact, in general, with the surrounding Ni and Fe atoms. This interaction leads to a decrease of the activation energy of the RDS (equation 2) as compared to their respective pristine materials, although sometimes the introduced SAs can also lead to a change in the RDS step.

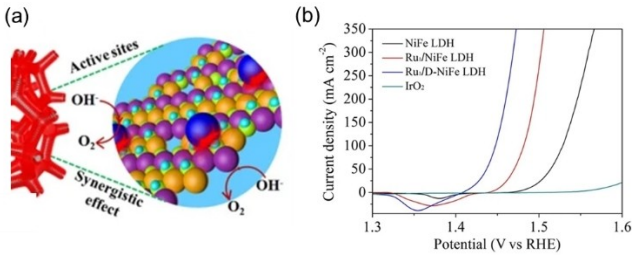

Figure 5. (a) Schematic representation of the Ru/defective-NiFe LDH. (b) LSV for OER under 1 M KOH of Ru doped defective NiFe LDH (blue curve), Ru doped non-defective NiFe-LDH (red curve), pristine NiFe-LDH (black curve), and commercial IrO_2 (green curve). Reproduced with permission.[38] Copyright 2021, Springer Nature.

4. Ligand Functionalization

The local structure, chemical environment and accessibility of a catalytic site play a key role in the tuning of its catalytic activity. All these features can be modified through ligand-functionalization of the NiFe oxide/hydroxide structure (see Figure 6a for the ligands discussed in this section).[84] Indeed, ligands can aid in the process of surface reconstruction that produces the catalytically active oxy(hydroxide) layer,[85] or can either stabilize the OER intermediates[86] and increase the catalytic selectivity.[87] Lastly, ligands with a large proton affinity can facilitate charge mobility in the systems, thus benefitting the overall kinetics of the sluggish OER process.

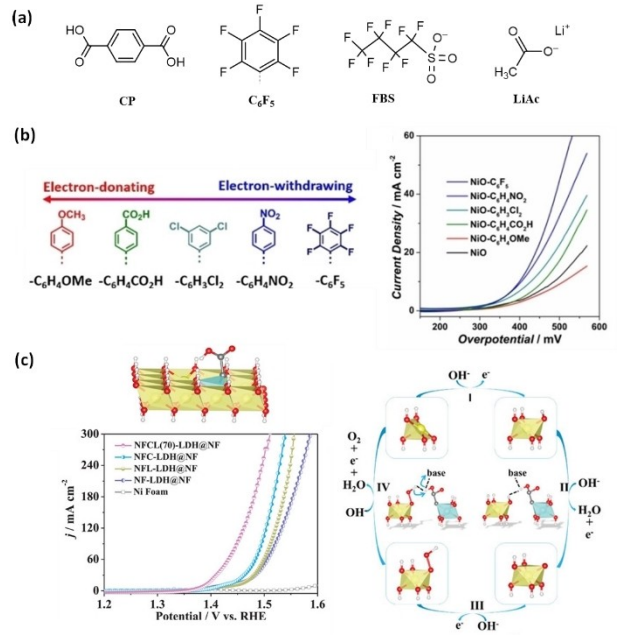

Figure 6. (a) Most relevant ligands discussed in this section. (b) Influence of the EWD and EDG effect of the ligands in the OER performance of ligand-modified NiO materials onto a glassy carbon electrode in 1 M KOH. Reproduced with permission.[45] Copyright 2020, Wiley-VCH. (c) LSV curves of several ligand-modified NiFe LDHs onto a Ni foam electrode in 1 M KOH with iR compensation of the as-prepared Li^+ doped and acetate intercalated (NFCL(70)- LDH @ NF), the pristine NiFe LDH (NF-LDH @ NF), the NiFe LDH with carboxylate ligand (NFC- LDH @ NF), the Li doped NiFe LDH (NFL-LDH @ NF) and the Ni foam support. On the right, the mechanistic OER pathway for the as-prepared Li^+ doped and acetate intercalated (NFCL(70)-LDH @ NF is shown. Reproduced with permission.[43] Copyright 2022, Wiley-VCH.

Carboxylate groups (Figure 5a, CP) have been shown to increase the activity of a Ni and Fe coordination polymer deposited on Ni foam (NiFeCP/NF) when used as an anode for OER (entry 13, Table 1).[46] In this case, the functionalization plays a double role. The carboxylate groups located at the first coordination sphere increase the oxidation state of the metal centers, while the uncoordinated ones (second coordination sphere) act as proton shuttles, delivering charges from the catalytic sites to the electrolyte. This phenomenon has also been reported and studied for molecular catalysts.[88]

The electron withdrawing (EWD)/electron donating (EDG) nature of the ligand (Figure 6b) is a major factor in determining the final activity (entry 14, Table 1) of a functionalized NiO catalyst (which contains Fe due the use of a non-purified electrolyte). EWD groups attract the electron density of the metallic centers, as is the case of the $-C_6F_5$ ligand (Figure 5a), resulting in more oxidized sites with an increased activity towards OER.[45] In the other extreme, EDG substituents produce more reduced metal centers and hinder the OER reaction.

Also, not only the chemical nature but also the positions occupied by the ligands in NiFe LDHs impacts on their OER catalytic activity. The surfactant nonafluoro-1-butanesulphonate (FBS, Figure 6a) can occupy the space between the layers of the NiFe LDHs and drastically increase their OER activity (entry 15, Table 1).[42] Intercalation of the ligands sterically increases the separation between layers, facilitating the access of the solvent to the metal centers, while the sulfonate group aid in the proton shuttling process, similarly to what has been observed for other alkaline substituents such as carboxylates, previously discussed.

Finally, some ligands can induce more than one effect at once, increasing the activity of NiFe oxide/hydroxides based catalysts through various coexisting pathways (entry 16, Table 1). Lithium acetate (LiAc) (Figure 6a) can be introduced during the synthesis of NiFe LDHs, resulting in a major OER activity improvement.[43] In this case, the Li^+ cations substitute the Ni^{2+} sites in the LDH structure, while the acetate anions accumulate in the interlayer space. The doping effect of Li^+ stabilizes some active OER intermediates, and, at the same time, the carboxylate anions facilitate the charge transfer (Figure 6c, right). This example shows the potential of coupling more than one strategy for perfecting OER catalysts.

In summary, the introduction of ligands on the surface or the interlayers (for the LDH examples) of NiFe oxides/hydroxides electrocatalysts is an attractive strategy to modulate both the electronic properties of the active sites as well as the second coordination sphere effects.

5. Summary and Outlook

All the examples described above demonstrate that atomically and molecularly modifying NiFe oxides/hydroxides is an attractive approach to rationally improve their activity towards OER. On the one hand, introducing both cationic and anionic vacancies lowers the activation energy of the RDS of the reaction (equation 2) and, at the same time, increases the metallic behavior of the materials due to the more continue density of states (Scheme 1). The introduction of atomic SAs as a doping strategy strongly influences the electronic properties of the Ni and Fe atoms in the materials (Scheme 1), thus provoking a lowering of the activation energy of the deprotonation step (equation 2) and enhancing the final performance of the materials. In addition, the SAs are also active towards OER, opening the door to new mechanistic pathways due to

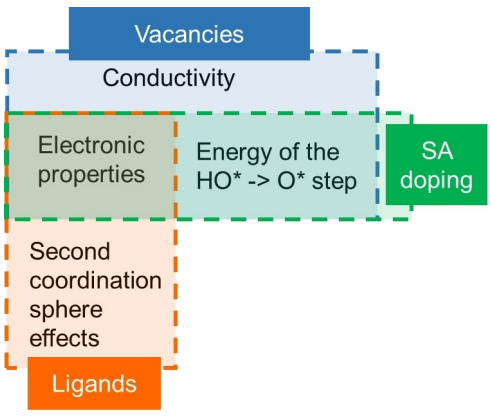

Scheme 1. Schematic representation of the effects of molecularly and atomically engineering NiFe oxides/hydroxides based electrocatalysts.

the synergy between the SAs and the NiFe oxide/hydroxide material. Most of the reported examples following this strategy are based on noble metal SAs. However, non-precious metals such as Cu and Mo have been successfully introduced as dopants on NiFe oxide/hydroxides in the form of small clusters/NPs[89] or as a third metal in the crystalline structure.[90,91] Consequently, exploring the use of non-precious metal-based SAs as dopants is a promising route to atomically tune the OER activity of NiFe oxide/hydroxides without the introduction of critical raw materials. Finally, the addition of a ligand in the NiFe oxide/hydroxide electrocatalyst (both on the surface and in the interlayer in the case of the LDH) has proven to be an effective strategy to induce second coordination sphere effects, especially important to accelerate the different proton coupled electron transfers taking place during the catalytic cycle (Scheme 1). In addition, by tuning the electronic properties of the ligand, the properties of the metal centers are also modified.

Traditionally, modifying the electronic properties and, in consequence, the binding energies of the reaction intermediates has been very challenging from the experimental point of view. However, currently, as demonstrated by these examples, this is possible by atomically and molecularly modifying the pristine materials. These modified NiFe oxides/hydroxides present an enhanced performance towards OER thanks to the rational tuning of their electronic and second coordination sphere properties. As stands out from Table 1, the best performing systems are those combing more than one strategy. For example, the system presenting the lower η_{10} overpotential[43] (entry 16) is the one that takes advantage of the strong electronic effect induced by the doping (in this case Li^+ cations) and the effect of the acetate as a shuttle for the proton electron transfer involved in the RDS (equation 2). Thanks to the synergistic effect of both modifications, the final NiFe oxide/hydroxide LDH presents one of the lowest reported overpotentials to achieve 10 mA/cm^2, 159 mV. By comparing the different effects (Table 1), one can see that using a ligand able to facilitate the proton transfer the η_{10} parameter can be substantially lowered. This strategy, which entails the use of ligands to functionalize the catalyst surface, has been more studied for reductive processes (i.e., proton and CO_2 reduction), and unfortunately remains almost unexplored regarding the water oxidation counterpart.[84] Thus, more research should be carried out to further exploit this powerful approach.

As recently published, combining more than one of these effects with other strategies, such as an increase of the surface area by preparing an amorphous material, leads to high performing NiFe LDHs. Zhao and co-workers reported the preparation of an ultrathin porous NiFe LDH with the presence of Ni(III) defects (Ni(II) oxidized to Ni(III)) and oxygen vacancies by a solvothermal method using H_2O_2.[36] The synergistic effect of the three modifications leads to an electrocatalyst with a η_{10} of 170 mV. Its porous nature increased the number of active sites, while the Ni(III) ions close to the oxygen vacancies modified the energetic barriers of the steps 2 and 3 (see equations 2 and 3), favoring the final oxygen production, as demonstrated by DFT calculations.

In general, the evolution of the different modifications over time should be carefully analyzed, since under catalytic conditions these can be strongly modified due to the harsh conditions of OER. This highlights the need to use operando spectroscopies to determine the fate of the different induced modifications.

In short, further improvements in the field of catalytic OER through the use of NiFe oxide/hydroxides will need to exploit the combination of the three different strategies explained in this Concept: the introduction of different vacancies to increase the metallic nature of the NiFe oxides/hydroxides, the use of SAs doping to strongly modify their electronic properties through strong metal-support interactions arising from interfacial bonding, and finally the addition of a ligand able to facilitate the different proton transfers. However, further steps towards a higher volume utilization (higher number of actives per geometric area) need to be taken for the use of these catalysts in commercial alkaline electrolyzers.[92]

Acknowledgements

Sustained support from MICINN, FEDER and AGAUR are gratefully acknowledged. Recent research projects and grants include PID2019-104171RB-I00-, PID2021-128197NA-I00, and TED2021-129237B-I00. L. F. is indebted to the Ramón y Cajal Program (RYC2018-025394-I Fellowship) and to the Royal Society of Chemistry (R20-8077 Research Fund). X. S. thanks ICREA for the ICREA Academia prize 2020. E. S. DS. acknowledges the Maria Zambrano fellowship (MAZAM 681136) from the UAB and the Spanish Ministry of Universities, funded by the European Union-Next-Generation EU. A. M. acknowledges the support of the predoctoral program AGAUR-FI ajuts (2023 FI-3 00065) Joan Oró of the Secretariat of Universities and Research of the Department of Research and Universities of the Generalitat of Catalonia and the European Social Plus Fund.

Conflict of Interests

The authors declare no conflict of interest.

Data Availability Statement

Data sharing is not applicable to this article as no new data were created or analyzed in this study.

Keywords: water oxidation · NiFe electrocatalysts · vacancies · single atoms · ligand functionalization

[1] S. Yin Tee, K. Yin Win, W. Siang Teo, L.-D. Koh, S. Liu, C. Peng Teng, M.-Y. Han, S. Y. Tee, K. Y. Win, L. Koh, S. Liu, C. P. Teng, M. Han, W. S. Teo, *Adv. Sci.* **2017**, *4*, 1600337.
[2] Z. Abdin, A. Zafaranloo, A. Rafiee, W. Mérida, W. Lipiński, K. R. Khalilpour, *Renew. Sust. Energ. Rev.* **2020**, *120*, 109620.

[3] S. Yoshino, T. Takayama, Y. Yamaguchi, A. Iwase, A. Kudo, *Acc. Chem. Res.* **2022**, *55*, 966–977.
[4] S. Nitopi, E. Bertheussen, S. B. Scott, X. Liu, A. K. Engstfeld, S. Horch, B. Seger, I. E. L. Stephens, K. Chan, C. Hahn, J. K. Nørskov, T. F. Jaramillo, I. Chorkendorff, *Chem. Rev.* **2019**, *119*, 7610–7672.
[5] H. Inoue, T. Shimada, Y. Kou, Y. Nabetani, D. Masui, S. Takagi, H. Tachibana, *ChemSusChem* **2011**, *4*, 173-179.
[6] C. R. Lhermitte, K. Sivula, *ACS Catal.* **2019**, *9*, 2007–2017.
[7] I. C. Man, H. Y. Su, F. Calle-Vallejo, H. A. Hansen, J. I. Martínez, N. G. Inoglu, J. Kitchin, T. F. Jaramillo, J. K. Nørskov, J. Rossmeisl, *ChemCatChem* **2011**, *3*, 1159–1165.
[8] A. J. Tkalych, H. L. Zhuang, E. A. Carter, *ACS Catal.* **2017**, *7*, 5329–5339.
[9] J. O. M. Bockris, T. Otagawa, *J. Phys. Chem.* **1983**, *87*, 2960–2971.
[10] J. Song, C. Wei, Z. F. Huang, C. Liu, L. Zeng, X. Wang, Z. J. Xu, *Chem. Soc. Rev.* **2020**, *49*, 2196–2214.
[11] A. Peugeot, C. E. Creissen, D. Karapinar, H. N. Tran, M. Schreiber, M. Fontecave, *Joule* **2021**, *5*, 1281–1300.
[12] C. C. L. McCrory, S. Jung, J. C. Peters, T. F. Jaramillo, *J. Am. Chem. Soc.* **2013**, *135*, 16977–16987.
[13] D. A. Corrigan, *J. Electrochem. Soc.* **1987**, *134*, 377–384.
[14] L. Trotochaud, J. K. Ranney, K. N. Williams, S. W. Boettcher, *J. Am. Chem. Soc.* **2012**, *134*, 17253–17261.
[15] J. Y. C. Chen, L. Dang, H. Liang, W. Bi, J. B. Gerken, S. Jin, E. E. Alp, S. S. Stahl, *J. Am. Chem. Soc.* **2015**, *137*, 15090–15093.
[16] M. Gorlin, J. F. De Araujo, H. Schmies, D. Bernsmeier, S. Dresp, M. Gliech, Z. Jusys, P. Chernev, R. Kraehnert, H. Dau, P. Strasser, *J. Am. Chem. Soc.* **2017**, *139*, 2070–2082.
[17] B. J. Trześniewski, O. Diaz-Morales, D. A. Vermaas, A. Longo, W. Bras, M. T. M. Koper, W. A. Smith, *J. Am. Chem. Soc.* **2015**, *137*, 15112–15121.
[18] L. Trotochaud, S. L. Young, J. K. Ranney, S. W. Boettcher, *J. Am. Chem. Soc.* **2014**, *136*, 6744–6753.
[19] L. Francàs, S. Corby, S. Selim, D. Lee, C. A. Mesa, R. Godin, E. Pastor, I. E. L. Stephens, K. S. Choi, J. R. Durrant, *Nat. Commun.* **2019**, *10*, 1–10.
[20] S. Anantharaj, S. Kundu, S. Noda, *Nano Energy* **2021**, *80*, 105514.
[21] Z. Qiu, C. W. Tai, G. A. Niklasson, T. Edvinsson, *Energy Environ. Sci.* **2019**, *12*, 572–581.
[22] Y. Xu, Y. Hao, G. Zhang, Z. Lu, S. Han, Y. Li, X. Sun, *RSC Adv.* **2015**, *5*, 55131–55135.
[23] N.-C. Lo, P.-C. Chung, W.-J. Chuang, S. C. N. Hsu, I.-W. Sun, P.-Y. Chen, *J. Electrochem. Soc.* **2016**, *163*, D9–D16.
[24] X. Lu, C. Zhao, *Nat. Commun.* **2015**, *6*, 1–7.
[25] J. R. Swierk, S. Klaus, L. Trotochaud, A. T. Bell, T. D. Tilley, *J. Phys. Chem. C* **2015**, *119*, 19022–19029.
[26] B. M. Hunter, W. Hieringer, J. R. Winkler, H. B. Gray, A. M. Müller, *Energy Environ. Sci.* **2016**, *9*, 1734–1743.
[27] M. W. Louie, A. T. Bell, *J. Am. Chem. Soc.* **2013**, *135*, 12329–12337.
[28] S. Dresp, F. Luo, R. Schmack, S. Kühl, M. Gliech, P. Strasser, *Energy Environ. Sci.* **2016**, *9*, 2020–2024.
[29] J. Y. C. Chen, L. Dang, H. Liang, W. Bi, J. B. Gerken, S. Jin, E. E. Alp, S. S. Stahl, *J. Am. Chem. Soc.* **2015**, *137*, 15090–15093.
[30] E. Coronado, J. R. Galén-Mascarós, C. Martí-Gastaldo, A. Ribera, E. Palacios, M. Castro, R. Burriel, *Inorg. Chem.* **2008**, *47*, 9103–9110.
[31] L. Gong, H. Yang, A. I. Douka, Y. Yan, B. Y. Xia, *Adv Sustain Syst* **2021**, *5*, 2000136.
[32] X. Li, Y. Liu, Q. Sun, Z. Huangfu, W.-H. Huang, Z. Wang, C.-C. Chueh, C.-L. Chen, Z. Zhu, *ACS Sustain Chem Eng* **2022**, *10*, 14474–14485.
[33] Q. Xie, Z. Cai, P. Li, D. Zhou, Y. Bi, X. Xiong, E. Hu, Y. Li, Y. Kuang, X. Sun, *Nano Res.* **2018**, *11*, 4524–4534.
[34] Y. Wang, M. Qiao, Y. Li, S. Wang, *Small* **2018**, *14*, 1800136.
[35] S. Liu, H. Zhang, E. Hu, T. Zhu, C. Zhou, Y. Huang, M. Ling, X. Gao, Z. Lin, *J Mater Chem A Mater* **2021**, *9*, 23697–23702.
[36] Z. Zhao, Q. Shao, J. Xue, B. Huang, Z. Niu, H. Gu, X. Huang, J. Lang, *Nano Res.* **2022**, *15*, 310–316.
[37] J. Zhang, J. Liu, L. Xi, Y. Yu, N. Chen, S. Sun, W. Wang, K. M. Lange, B. Zhang, *J. Am. Chem. Soc.* **2018**, *140*, 3876–3879.
[38] P. Zhai, M. Xia, Y. Wu, G. Zhang, J. Gao, B. Zhang, S. Cao, Y. Zhang, Z. Li, Z. Fan, C. Wang, X. Zhang, J. T. Miller, L. Sun, J. Hou, *Nat. Commun.* **2021**, *12*, 4587.
[39] W. Chen, B. Wu, Y. Wang, W. Zhou, Y. Li, T. Liu, C. Xie, L. Xu, S. Du, M. Song, D. Wang, Y. Liu, Y. Li, J. Liu, Y. Zou, R. Chen, C. Chen, J. Zheng, Y. Li, J. Chen, S. Wang, *Energy Environ. Sci.* **2021**, *14*, 6428–6440.
[40] X. Duan, P. Li, D. Zhou, S. Wang, H. Liu, Z. Wang, X. Zhang, G. Yang, Z. Zhang, G. Tan, Y. Li, L. Xu, W. Liu, Z. Xing, Y. Kuang, X. Sun, *Chem. Eng. J.* **2022**, *446*, 136962.
[41] L. Wang, L. Zhang, W. Ma, H. Wan, X. Zhang, X. Zhang, S. Jiang, J. Y. Zheng, Z. Zhou, L. Wang, L. Zhang, W. Ma, H. Wan, X. J. Zhang, X. Zhang, S. Jiang, J. Y. Zheng, Z. Zhou, *Adv. Funct. Mater.* **2022**, *32*, 2203342.
[42] W. Li, F. Li, Y. Zhao, C. Liu, Y. Li, H. Yang, K. Fan, P. Zhang, Y. Shan, L. Sun, *Sci. Chi. Chem.* **2021**, *65*, 382–390.
[43] X. Lin, S. Cao, X. Chen, H. Chen, Z. Wang, H. Liu, H. Xu, S. Liu, S. Wei, X. Lu, X. Lin, S. Cao, X. Chen, Z. Wang, H. Liu, H. Xu, S. Liu, X. Lu, H. Chen, S. Wei, *Adv. Funct. Mater.* **2022**, *32*, 2202072.
[44] X. Luo, X. Wei, H. Zhong, H. Wang, Y. Wu, Q. Wang, W. Gu, M. Gu, S. P. Beckman, C. Zhu, *ACS Appl. Mater. Interfaces* **2020**, *12*, 3539–3546.
[45] L. Fan, B. Zhang, Z. Qiu, N. V. R. A. Dharanipragada, B. J. J. Timmer, F. Zhang, X. Sheng, T. Liu, Q. Meng, A. K. Inge, T. Edvinsson, L. Sun, *ChemSusChem* **2020**, *13*, 5901–5909.
[46] W. Li, F. Li, H. Yang, X. Wu, P. Zhang, Y. Shan, L. Sun, *Nat. Commun.* **2019**, *10*, 1–11.
[47] F. Liao, X. Zhao, G. Yang, Q. Cheng, L. Mao, L. Chen, *J. Alloys Compd.* **2021**, *872*, 159649.
[48] J. Mohammed-Ibrahim, *J. Power Sources* **2020**, *448*, 227375.
[49] D. Friebel, M. W. Louie, M. Bajdich, K. E. Sanwald, Y. Cai, A. M. Wise, M. J. Cheng, D. Sokaras, T. C. Weng, R. Alonso-Mori, R. C. Davis, J. R. Bargar, J. K. Nørskov, A. Nilsson, A. T. Bell, *J. Am. Chem. Soc.* **2015**, *137*, 1305–1313.
[50] W. Cai, R. Chen, H. Yang, H. B. Tao, H. Y. Wang, J. Gao, W. Liu, S. Liu, S. F. Hung, B. Liu, *Nano Lett.* **2020**, *20*, 4278–4285.
[51] Y. Wang, Y. Zhou, M. Han, Y. Xi, H. You, X. Hao, Z. Li, J. Zhou, D. Song, D. Wang, F. Gao, *Small* **2019**, *15*, 1805435.
[52] L. Xu, F. T. Zhang, J. H. Chen, X. Z. Fu, R. Sun, C. P. Wong, *ACS Appl Energy Mater* **2018**, *1*, 1210–1217.
[53] C. Peng, N. Ran, G. Wan, W. Zhao, Z. Kuang, Z. Lu, C. Sun, J. Liu, L. Wang, H. Chen, *ChemSusChem* **2020**, *13*, 811–818.
[54] J. Chen, F. Zheng, S. J. Zhang, A. Fisher, Y. Zhou, Z. Wang, Y. Li, B. Bin Xu, J. T. Li, S. G. Sun, *ACS Catal.* **2018**, *8*, 11342–11351.
[55] Y. Xue, Z. S. Fishman, J. A. Röhr, Z. Pan, Y. Wang, C. Zhang, S. Zheng, Y. Zhang, S. Hu, *J. Mater. Chem. A* **2018**, *6*, 21918–21926.
[56] J. Zhou, L. Yu, Q. Zhu, C. Huang, Y. Yu, *J. Mater. Chem. A* **2019**, *7*, 18118–18125.
[57] Q. Zhou, T. T. Li, J. Qian, W. Xu, Y. Hu, Y. Q. Zheng, *ACS Appl. Energy Mater.* **2018**, *1*, 1364–1373.
[58] C. Liang, P. Zou, A. Nairan, Y. Zhang, J. Liu, K. Liu, S. Hu, F. Kang, H. J. Fan, C. Yang, *Energy Environ. Sci.* **2020**, *13*, 86–95.
[59] W. E. Org, H. Wei, J. Liu, Y. Deng, W. Hu, C. Zhong, *Int. J. Electrochem. Sci.* **2019**, *14*, 4173–4184.
[60] Y. Gu, Y. Wang, W. An, Y. Men, Y. Rui, X. Fan, B. Li, *New J. Chem.* **2019**, *43*, 6555–6562.
[61] L. Su, H. Du, C. Tang, K. Nan, J. Wu, C. Ming Li, *J. Colloid Interface Sci.* **2018**, *528*, 36–44.
[62] D. Zhou, Z. Cai, Y. Bi, W. Tian, M. Luo, Q. Zhang, Q. Xie, J. Wang, Y. Li, Y. Kuang, X. Duan, M. Bajdich, S. Siahrostami, X. Sun, *Nano Res.* **2018**, *11*, 1358–1368.
[63] N. Wang, Z. Cao, X. Kong, J. Liang, Q. Zhang, L. Zheng, C. Wei, X. Chen, Y. Zhao, L. Cavallo, B. Zhang, X. Zhang, *J. Mater. Chem. A* **2018**, *6*, 16959–16964.
[64] Y. Xu, Y. Hao, G. Zhang, Z. Lu, S. Han, Y. Li, X. Sun, *RSC Adv.* **2015**, *5*, 55131–55135.
[65] S. Li, J. Liu, S. Duan, T. Wang, Q. Li, *Chi. J. Catal.* **2020**, *41*, 847–852.
[66] J. Liu, Y. Liu, X. Mu, H. Jang, Z. Lei, S. Jiao, P. Yan, M. G. Kim, R. Cao, *Adv. Funct. Mater.* **2022**, *32*, 2204086.
[67] D. Zhou, Z. Cai, Y. Jia, X. Xiong, Q. Xie, S. Wang, Y. Zhang, W. Liu, H. Duan, X. Sun, *Nanoscale Horiz.* **2018**, *3*, 532–537.
[68] X. Zhang, Y. Zhao, Y. Zhao, R. Shi, G. I. N. Waterhouse, T. Zhang, *Adv. Energy Mater.* **2019**, *9*, 1900881.
[69] K. Zhu, F. Shi, X. Zhu, W. Yang, *Nano Energy* **2020**, *73*, 104761.
[70] G. Zhang, J. Yuan, Y. Liu, W. Lu, N. Fu, W. Li, H. Huang, *J. Mater. Chem. A* **2018**, *6*, 10253–10263.
[71] L. Peng, N. Yang, Y. Yang, Q. Wang, X. Xie, D. Sun-Waterhouse, L. Shang, T. Zhang, G. I. N. Waterhouse, *Angew. Chem. Int. Ed.* **2021**, *60*, 24612–24619.
[72] Y. Zhao, X. Zhang, X. Jia, G. I. N. Waterhouse, R. Shi, X. Zhang, F. Zhan, Y. Tao, L. Z. Wu, C. H. Tung, D. O'Hare, T. Zhang, *Adv. Energy Mater.* **2018**, *8*, 1703585.
[73] Y. Zhou, W. Zhang, J. Hu, D. Li, X. Yin, Q. Gao, *ACS Sustain. Chem. Eng.* **2021**, *9*, 7390–7399.
[74] T. Tian, M. Zheng, J. Lin, X. Meng, Y. Ding, *Chem. Commun.* **2019**, *55*, 1044–1047.

[75] S. Wang, X. Ge, C. Lv, C. Hu, H. Guan, J. Wu, Z. Wang, X. Yang, Y. Shi, J. Song, Z. Zhang, A. Watanabe, J. Cai, *Nanoscale* **2020**, *12*, 9557–9568.
[76] M. Asnavandi, Y. Yin, Y. Li, C. Sun, C. Zhao, *ACS Energy Lett.* **2018**, *3*, 1515–1520.
[77] D. Zhou, X. Xiong, Z. Cai, N. Han, Y. Jia, Q. Xie, X. Duan, T. Xie, X. Zheng, X. Sun, X. Duan, *Small Met.* **2018**, *2*, 1800083.
[78] Q. Xu, H. Jiang, X. Duan, Z. Jiang, Y. Hu, S. W. Boettcher, W. Zhang, S. Guo, C. Li, *Nano Lett.* **2021**, *21*, 492–499.
[79] H. Kim, J. Kim, S. H. Ahn, *J. Ind. Eng. Chem.* **2019**, *72*, 273–280.
[80] A. Zhang, Y. Liang, H. Zhang, Z. Geng, J. Zeng, *Chem. Soc. Rev.* **2021**, *50*, 9817–9844.
[81] B. Qiao, A. Wang, X. Yang, L. F. Allard, Z. Jiang, Y. Cui, J. Liu, J. Li, T. Zhang, *Nat. Chem.* **2011**, *3*, 634–641.
[82] X. Zheng, J. Tang, A. Gallo, J. A. G. Torres, X. Yu, C. J. Athanitis, E. M. Been, P. Ercius, H. Mao, S. C. Fakra, C. Song, R. C. Davis, J. A. Reimer, J. Vinson, M. Bajdich, Y. Cui, *Proc. Natl. Acad. Sci. USA* **2021**, *118*, e2101817118.
[83] J. Yan, L. Kong, Y. Ji, J. White, Y. Li, J. Zhang, P. An, S. Liu, S. T. Lee, T. Ma, *Nat. Commun.* **2019**, *10*, 1–10.
[84] G. Martí, L. Mallón, N. Romero, L. Francàs, R. Bofill, K. Philippot, J. García-Antón, X. Sala, *Adv. Energy Mater.* **2023**, *2300282*, 1–25.
[85] T. Wu, S. Sun, J. Song, S. Xi, Y. Du, B. Chen, W. A. Sasangka, H. Liao, C. L. Gan, G. G. Scherer, L. Zeng, H. Wang, H. Li, A. Grimaud, Z. J. Xu, *Nat Catal 2019* **2019**, *2*, 763–772.
[86] L. Zhuang, Y. Jia, H. Liu, Z. Li, M. Li, L. Zhang, X. Wang, D. Yang, Z. Zhu, X. Yao, *Angew. Chem. Inter. Ed.* **2020**, *59*, 14664–14670.
[87] K. S. Exner, J. Anton, T. Jacob, H. Over, *ChemElectroChem* **2015**, *2*, 707–713.
[88] R. Matheu, M. Z. Ertem, J. Benet-Buchholz, E. Coronado, V. S. Batista, X. Sala, A. Llobet, *J. Am. Chem. Soc.* **2015**, *137*, 10786–10795.
[89] Y. Ma, K. Wang, D. Liu, X. Yang, H. Wu, C. Xiao, S. Ding, *J. Mater. Chem. A* **2019**, *7*, 22889–22897.
[90] J. Guo, K. Wang, H. Zhang, H. Zhang, *ACS Appl. Nano Mater.* **2023**, *6*, 379–389.
[91] Y. Gan, Z. Li, Y. Ye, X. Dai, F. Nie, X. Yin, Z. Ren, B. Wu, Y. Cao, R. Cai, X. Zhang, W. Song, *ChemSusChem* **2022**, *15*, e202201205.
[92] Z. Yu, Y. Bai, G. Tsekouras, Z. Cheng, C. Ying Bai, *Nano Select* **2022**, *3*, 766–791.

Manuscript received: July 14, 2023
Accepted manuscript online: September 13, 2023
Version of record online: ■■, ■■

CONCEPT

NiFe materials are the state-of-the-art electrocatalysts for water oxidation, therefore, fine tuning their properties is the cornerstone to achieving more active and efficient catalysts. In this concept, we will review the recently emerged strategies to engineer them molecularly and atomically by introducing different vacancies, incorporating single atoms or by ligand functionalization.

Atomic and molecular engineering

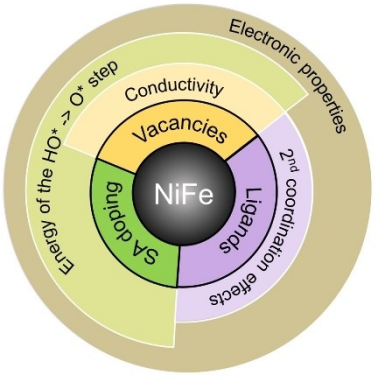

*Dr. E. S. Da Silva, A. Macili, Dr. R. Bofill, Dr. J. García-Antón, Dr. X. Sala, Dr. L. Francàs**